Research Article

Qi Dong[#], Sunfang Chen[#], Jiuqin Zhou[#], Jingcheng Liu, Yubin Zou, Jiawei Lin, Jun Yao, Dan Cai, Danhua Tao*, Bing Wu*, and Bin Fang*

Design of functional vancomycin-embedded bioderived extracellular matrix hydrogels for repairing infectious bone defects

https://doi.org/10.1515/ntrev-2022-0524 received September 4, 2022; accepted January 13, 2023

Abstract: The treatment of infectious bone defects has become a troublesome issue in orthopedics. The disease requires effective anti-infective and bone-reconstruction therapeutic functionalities. In this study, we prepared a novel antibacterial material (vancomycin-impregnated periosteal extracellular matrix [Van-PEM]) by embedding vancomycin in a periosteal extracellular matrix (PEM)derived hydrogel via physical stirring for the treatment of infectious bone defects. The microstructure, porosity, degradation, and release properties of this antibacterial hydrogel were characterized. The in vitro hemolytic reaction, cytotoxicity, osteogenic ability, and antibacterial properties were also carefully studied. The results showed that the Van-PEM hydrogel possessed a fibrous network structure with high porosity. Moreover, the hydrogel demonstrated slow degradation in vitro and could release vancomycin for at least 1 week. The hydrogel showed no cytotoxicity and possessed good biocompatibility with blood cells. It also promoted osteogenesis and exerted a significant bactericidal effect. Subsequently, the anti-infection and bone-healing abilities of the antibacterial hydrogel were investigated in a rat model of infectious calvarial defects, and the infectious skull defect was successfully cured in vivo. Therefore, Van-PEM hydrogels may represent a promising therapeutic approach for treating infectious bone defects.

Keywords: infectious bone defects, decellularized periosteum matrix hydrogel, anti-microbial

bone marrow mesenchymal stem cells

alkaline phosphatase

analysis of variance

cellular matrix

Abbreviations

ALP

ANOVA

BMSCs

# These authors contributed equally to this work and should be considered first co-authors.	21.10 00	Some marrow meconery mar stem come
	CCK-8	cell counting kit-8
	CCM	colony count method
	DAPI	4',6-diamino-2-phenylindole staining
	DMEM	Dulbecco's modified Eagle's medium
* Corresponding author: Danhua Tao, Department of Pathology, The	EDS	energy-dispersive X-ray spectroscopy
Central Hospital Affiliated to Shaoxing University, Shaoxing,	FTIR	Fourier transform infrared spectra
312030, China, e-mail: taodanhua85@qq.com	GAPDH	glyceraldehyde-3-phosphate dehydrogenase
* Corresponding author: Bing Wu, Department of Spine Surgery,	H&E	hematoxylin and eosin staining
The Central Hospital Affiliated to Shaoxing University, Shaoxing,	MRSA	methicillin-resistant Staphylococcus aureus
312030, China, e-mail: wubing@usx.edu.cn * Corresponding author: Bin Fang, Department of Spine Surgery,	OCM	Oxford cup method
The Central Hospital Affiliated to Shaoxing University, Shaoxing,	OD	optical density
312030, China, e-mail: fangbin@usx.edu.cn	PBS	phosphate-buffered saline
Qi Dong: Department of Osteology, Honghui Hospital, Xi'an Jiao	PEM	periosteal extracellular matrix
Tong University, Xi'an City, 710054, China	qPCR	quantitative polymerase chain reaction
Sunfang Chen, Jingcheng Liu, Yubin Zou, Jiawei Lin, Jun Yao,	SEM	scanning electron microscopy
Dan Cai: Department of Spine Surgery, The Central Hospital Affiliated to Shaoxing University, Shaoxing, 312030, China	TBS	tris-buffered saline
liuqin Zhou: Department of Infectious Disease, Shengjing Hospital	Van-PEM	vancomycin-impregnated periosteal extra-

S Jiuqin Zhou: Department of Infectious Disease, Shengjing Hospital of China Medical University, Shenyang, 110000, China

³

Tł 3

Th 31

1 Introduction

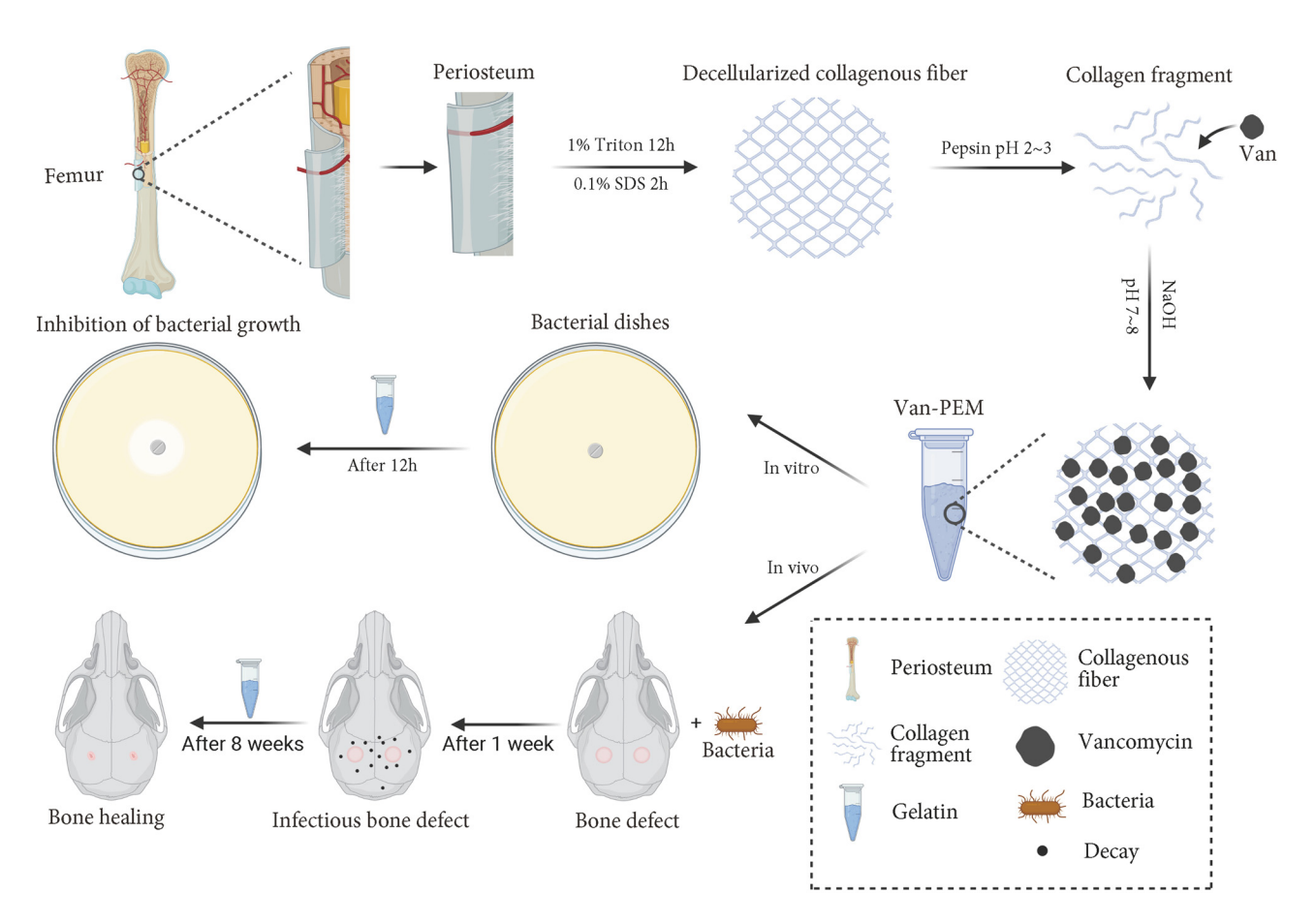
Infectious bone defects caused by osteomyelitis and open fracture infections are difficult to heal [1,2]. Staphylococcus aureus is the most common causative agent of bone infections [3]. Although bone tissue possesses remarkable regeneration and repair capabilities, when infections and bone defects reach a critical size, a bone repair can no longer proceed spontaneously [4]. Bone transplantation is the most commonly used technique for repairing bone defects. This technique repairs bone defects through the formation of new bone and the degradation of the transplanted bone (crawling replacement process). The key to the success of bone transplantation lies in a sterile and well-vascularized host bed. Orthopedic surgeons typically use repeated debridement and prolonged systemic antibiotic therapy to control bone defect wound infections [5,6]. In recent years, the local use of antibiotics has become a hot topic in the treatment of bone infections because this technique can maintain an effective antibacterial concentration while reducing antibiotic resistance and systemic toxicity. The usage of topical antibiotic-carrying cement with systemic antibiotics has become the main treatment strategy for bone infectious defects. Recently, biodegradable bone substitutes have been used to provide local antibacterial and osteogenic effects [7], with the expectation of a shift from multi-stage treatment to single-stage treatment.

Biodegradable bone substitutes, including bioactive glass, hydroxyapatite, and tricalcium phosphate, have been the focus of several studies [8-12]. Anti-microbial agents can be loaded into bone substitutes using various methods, including electrostatic adsorption, porous physical adsorption, nano-encapsulation, microsphere encapsulation, and chemical cross-linking [8,11–14]. Currently, antibiotics and metallic nanosilver are the most commonly used antimicrobials [15] to achieve antibacterial activity. However, several challenges remain. First, most bone substitutes require surface modification before binding to antibacterial agents, often with toxic crosslinking agents such as glutaraldehyde [8]. Second, bone substitutes must be capable of both bone induction and conduction [16]. Currently, most bone substitutes are non-bioactive materials, and the bone induction and conduction effects are usually much lower than those of bioactive bone substitutes and may be weakened in an infected environment [5]. Finally, Ag is cytotoxic and is not conducive to tissue repair and osteogenesis. In addition, its accumulation in the body may increase the burden on the liver and kidneys [11].

Bioactive materials, especially type I collagen, which is a major component of the bone extracellular matrix, have been studied as bone substitutes because of their unparalleled biocompatibility with non-biomaterials and their ability to simulate the cellular microenvironment and stimulate and support cell proliferation [17]. Tissue cell matrix material that retains the natural internal three-dimensional framework, a large number of protein structures, growth factors, and other active ingredients can retain the native microenvironment of the cell to a great extent and maintain its original features, leading to cell adhesion, proliferation, and differentiation along with promoting tissue repair and regeneration. These advantages cannot be achieved using the current synthetic materials [18]. This three-dimensional structure can also provide bone conduction to host capillaries and bone progenitor cells [6]. Cellular tissue-derived hydrogels can also retain complex biochemical components and assemble to form nanofibrous scaffolds. These scaffolds can recruit surrounding cells to migrate to the scaffolds, attach to the collagen fibers within the scaffolds, grow in parallel, and then replace by regenerative tissue [19-21].

The periosteum is a connective tissue envelope covering the surface of the bone and contains many growth factors, such as BMP-2, IGF-1, and TGF-β. These factors have strong bone induction abilities and play a critical role in the bone repair process [22]. In addition, the periosteum is rich in collagen, which promotes osteoblast differentiation and formation of mineralized nodules [23], which is the basic structural unit of natural bone [24]. It has been demonstrated that acellular periosteum scaffolds can promote bone defect regeneration and ectopic ossification [25-27]. In our previous study, we decellularized the periosteum and prepared it into a hydrogel, which could enhance osteogenesis, osteogenic differentiation, and biological bone mineralization, thus making it suitable for bone defect repair [28]. Antibiotics can be soaked and physically embedded in collagen hydrogels for functional applications [29,30]. However, the effect of vancomycinloaded extracellular matrix hydrogels on the repair of infectious bone defects requires further investigation.

In this study, vancomycin was physically encapsulated in an acellular perichondrium hydrogel to prepare a novel material with antibacterial and osteogenic properties (Scheme 1). Since the filamentous collagen fibers that make up the gel had the characteristics of micro–nanostructure, the porous structure composed of them was more in favor of drug loading. The vancomycin-impregnated periosteal extracellular matrix (Van-PEM) hydrogel exhibited satisfactory longacting bactericidal, biocompatible, and osteogenic properties. The antibacterial and bone-healing abilities of the Van-PEM hydrogel were verified *in vitro* and *in vivo*, suggesting that the Van-PEM hydrogel possesses potential as an antibacterial bone substitute for use in treating infectious bone defects.



Scheme 1: Schematic showing application of the porcine-acellular-periosteal-matrix hydrogel-encapsulated vancomycin to heal infectious bone defects.

2 Materials and methods

2.1 Materials

Triton X-100 solution and sodium dodecyl sulfate were purchased from Sinopharm Chemical Reagents Co., Ltd. Giemsa stain, pepsin, and Masson's trichrome staining kits were purchased from Beijing Solarbio Science & Technology Co., Ltd. Alkaline phosphatase (ALP) assay kit was purchased from Nanjing Jiancheng Bioengineering Institute Co., Ltd. Lutein was purchased from Yeasen Biotech Co., Ltd.

2.2 Synthesis of the Van-PEM hydrogel

The periosteum was removed from the femur surface of an adult pig sourced from a local abattoir. Three freeze–thaw cycles (–80 to 37°C) were performed after removing the stains on the periosteum surface; then, the periosteum was cut into appropriate size after removing other tissues on the surface with scissors. The periosteum was placed in a

1% Triton solution, and the rotation speed was adjusted to 120 rpm for 12 h, then placed in a 1% sodium dodecyl sulfate solution at the same speed for 2h, and rinsed with flowing phosphate-buffered saline (PBS) buffer for 12 h. The tissue was ground into a powder after freeze-drying overnight, and 20 mg/mL periosteum powder was slowly added to the solution containing pepsin and vigorously stirred, and the pH of the solution was adjusted to approximately 1.5. Vancomycin was added to the solution and stirred evenly to achieve a concentration of 2 mg/mL vancomycin. The solution was digested on a shaking table for 2h until the periosteum powder was fully dissolved. The solution was stored at 4°C for 2 weeks. For use, 10× PBS solution and sodium hydroxide solutions were added to adjust the pH to 7–8. The solid hydrogel was prepared after the solution was incubated at 37°C for approximately 5 min.

2.3 Porosity

Two methods were used to measure the porosities of the PEM and Van-PEM hydrogels. The first method was the medium-immersion method. After the hydrogel was placed at -80° C for 1 h, it was freeze-dried overnight. We weighed (W_1) the freeze-dried hydrogel, saturated it with isopropyl alcohol, removed the lyophilized gel, wiped the isopropyl alcohol from the surface, and reweighed the sample (W_2) . An appropriate volume of isopropyl alcohol (V_1) was added to a calibrated test tube, soaked lyophilized gel was gently added to the test tube, and the volume (V_2) was recorded. The porosity was calculated as follows:

Porosity =
$$(W_2 - W_1)/(V_2 - V_1) \times \rho$$
,

where ρ is the density of isopropyl alcohol. The second method used to measure the porosity was to scan the sample section with scanning electron microscopy (SEM) and calculate the gel porosity using ImageI software.

2.4 In vitro degradation performance

The PEM and Van-PEM hydrogels were weighed and placed in a solution containing collagenase I (5 U/mL) for 21 days at 37°C. The enzyme solution was changed every 3 days. Samples were weighed for degradation at 7, 14, and 21 days. The samples were washed with PBS before weighing to remove enzyme solution. The remaining mass after degradation was quantified by dividing the weight degraded by the original weight. The degradation of PEM and Van-PEM hydrogels in PBS without collagen protease I was tested using the aforementioned method. The PBS solution containing collagen protease I was replaced with the PBS solution, and the degradation of PEM and Van-PEM hydrogels was tested again as described above. Finally, the pH of the PBS solution was adjusted to 5, and the aforementioned steps were repeated to test the degradation of the PEM and Van-PEM hydrogels in an acidic PBS solution.

2.5 Release of vancomycin from the Van-PEM hydrogel

To determine the release of vancomycin, a series of vancomycin solutions with varying concentrations was prepared, and the absorbance values were measured using a UV spectrophotometer to create a standard curve (Y = 1.8068x + 0.1092, $R^2 = 0.996$). Then, the PEM and Van-PEM hydrogels were placed in centrifuge tubes, 1 mL of PBS solution was added, and the tubes were placed in a 37°C thermostat. PBS solution was removed at specific time intervals. After the dissolved hydrogel was removed by centrifugation, a release curve was constructed from the optical

density (OD) measured at 281 nm. The release behavior of PEM hydrogels containing 1, 4, and 7 mg/mL vancomycin was tested in a PBS solution. In addition, the release performance of PEM hydrogels containing 2 mg/mL vancomycin was investigated in PBS, PBS containing collagen protease I, and acidic PBS.

2.6 Antibacterial properties in vitro

The antibacterial properties of the Van-PEM hydrogels were determined using the Oxford cup method (OCM). Representative gram-positive (S. aureus and Enterococcus faecalis) and gram-negative bacteria (Escherichia coli) were selected for the experiment. First, a single colony of bacteria was placed in a test tube containing a liquid medium, and the test tube was placed in a shaker with a speed of 150 rpm and a temperature of 37°C overnight. A certain volume of bacteria in the test tube was selected and diluted until the OD value was $0.1 (0-1.5 \times 10^8 \text{ UFC/L})$. The bacteria and medium (50-60°C) were thoroughly mixed and added to a Petri dish, where the volume ratio of bacteria and medium was 1:10. When the medium cooled and became solid, an Oxford cup was used to make two identical wells in the medium, and the same volume of PEM and Van-PEM hydrogels was added to the wells, and the Petri dishes were placed in the bacterial incubator. The diameter of the sterile circle around the hydrogel was measured and recorded after 12 h. The antibacterial effects of the PEM and Van-PEM hydrogels soaked in PBS for 7, 14, and 21 days were also tested using the aforementioned method.

Subsequently, *S. aureus* was used for colony count method (CCM) detection. First, the PEM and Van-PEM hydrogels were cut into small pieces, placed in test tubes, and sterilized under UV light for 6 h. After adding the same volume of medium containing *S. aureus* (10^8 UFC/L) to the test tube, the test tube was placed on a shaker, and the conditions were set as described above. At 6 and 12 h, $20~\mu L$ of bacterial suspensions of the same ratio was removed and incubated on a nutrient agar plate at $37^{\circ}C$ for 24 h, after which the bacteria on the plate were counted.

2.7 Cytotoxicity and hemolysis test

Hundred microliters of PEM hydrogel and Van-PEM hydrogel were added to a 24-well plate for irradiation (25 kg, γ -radiation) sterilization. Bone marrow mesenchymal stem cells

(BMSCs) were seeded in the empty wells, and wells with PEM hydrogels, and Van-PEM hydrogels at a density of 4×10^4 cells/hole. Dulbecco's modified Eagle's medium (DMEM; Hyclone) containing 10% (v/v) fetal bovine serum, 100 µg/mL penicillin, and 100 µg/mL streptomycin was added to the culture wells. The cells were cultured at 37°C in a humid environment containing 5% carbon dioxide. After co-culturing for 48 h, the cells were stained with calophyllum staining kit for living cells and observed under a fluorescence microscope at 515 nm wavelength.

Cell counting kit-8 (CCK8) was used to detect the cytotoxicity of the PEM and Van-PEM hydrogels, PEM and Van-PEM hydrogels were soaked in DMEM (the volume of hydrogel/the volume of culture medium is 1:5), the supernatant as 100% leaching solution was collected, and then mixed with a proportion of DMEM cell culture to obtain the culture solution containing 0, 20, 50, and 100% leaching solution for further experiments. Mesenchymal stem cells (MSCs) were inoculated into 96-well plates at a density of 2,000 cells per well. After incubation at 37°C for 24 h, the supernatant medium was removed from each well, 100 uL of medium containing different proportions of leachate was added, and DMEM without leachate was used as a control group. On days 1, 3, and 5, respectively, 10 µL of DMEM cell culture containing CCK8 reagent was added to each well and incubated at 37°C for 1 h, then measured with a spectrophotometer at 450 nm wavelength.

Hemolysis of the PEM and Van-PEM hydrogels was evaluated using a previously reported method [31]. One milliliter of blood collected from volunteers was added to a sterile Eppendorf tube and centrifuged at 850g for 5 min. The supernatant was discarded, and the red blood cells were rinsed several times with isotonic sterile PBS solution. The rinsed red blood cells were then suspended in Eppendorf tubes containing deionized water and PBS. PEM and Van-PEM hydrogels were added to the erythrocyte suspension, incubated at 37°C for 60 min, and centrifuged for 5 min. The absorbance of the supernatant was measured at 540 nm, and the hemolysis rate was calculated. Eppendorf tubes containing deionized water were used as positive controls, and Eppendorf tubes containing PBS were used as negative controls. The percentage of hemolysis was calculated using the following formula: (OD of sample - OD of negative control)/OD of positive control \times 100.

2.8 Osteogenesis tests

The ALP activity of the MC3T3-E1 cells was monitored using an ALP assay kit. The PEM and Van-PEM hydrogels

were irradiated after being placed in a 24-well plate. MC3T3-E1 cells were seeded in 20 mg/mL PEM and Van-PEM hydrogels. The cells were first incubated in DMEM for 24 h and then replaced with osteoblast induction medium, which included 100 nM dexamethasone, 5 µM ascorbic acid, and 1 mM B-glycerophosphate. On days 3 and 7, the ALP activity of MC3T3-E1 cells in different samples was measured according to the manufacturer's instructions.

ALP staining was used to detect ALP expression. MC3T3-E1 cells (1 \times 10⁵) were placed in 24-well plates containing PEM and Van-PEM hydrogels. The osteoblast induction medium was changed every 2 days and incubated at 37°C for 7 days for staining. The samples were lightly cleaned three times with Tris-buffered saline (TBS) solution and fixed with 4% paraformaldehyde at 37°C. An ALP staining kit was used for staining and observation after 12 h.

Quantitative polymerase chain reaction (qPCR) analysis was used to detect the expression of genes related to osteogenesis. MC3T3-E1 cells were seeded in 24-well plates containing 20 mg/mL PEM hydrogel or Van-PEM hydrogel at a density of 1×10^5 cells/well. Wells lacking hydrogel substrates were used as negative controls, qPCR was performed on day 14 for Runx2, OSX, and OCN. The cells were then stained with ALP. PCR was performed using the standard method for each target gene, standardized by glyceraldehyde-3-phosphate dehydrogenase (GAPDH), and calculated using the $2^{-\Delta\Delta Ct}$ method. Primer sequences for each gene are listed in Table S1.

2.9 *In vivo* experiments

2.9.1 Model of infectious bone defects

Male SD rats weighing 200-300 g were selected for animal experiments. All animal experiments were approved by the Institutional Animal Care and Use Committee (IACUC) of the Zhejiang Center of Laboratory Animals (ZJCLA). The following procedure was used to create infectious bone defects in rat skulls. After the rats were completely anesthetized, hair on the surface of the skull was removed using a shaving machine, and the skin was disinfected with 75% alcohol. The skull was exposed after the skin was cut, and a 4 mmdiameter defect was created in the middle of the skull by turning the head [32]. The head was continuously immersed in sterile saline during the surgery. The defect site was soaked in 100 µL of methicillin-resistant S. aureus (MRSA) at 108 CFU/mL, after which collagen plugs were resorbed (REF 260-509-400, Bicon, USA) to cover each defect and create an infectious bone defect model. The experimental rats were divided into three groups with four rats in each group. In the first group, no bacteria or hydrogel was added to the skull defect, whereas in the second group, only MRSA was added to the skull defect; in the third group, MRSA and the prefabricated gel with a diameter of 4 mm and a height of 3 mm were added to the skull defect. Absorbable sutures were used to suture the cranial membrane and skin.

2.9.2 In vivo sterilization evaluation

The skull was collected 1 week after surgery and scanned using micro-CT (Hiscan XM) to observe the preparation of the bone infection model. At Weeks 5 and 9, $2\,\mathrm{mm}\times1\,\mathrm{mm}$ tissue was cut from the skull defects of rats. The samples were placed in normal saline and stirred for 10 min. Twenty microliters of the above mixture were absorbed and inoculated onto a bacterial Petri dish. After the dishes were placed in a bacterial incubator for 24 h, the number of colonies on the dishes was observed and recorded.

2.9.3 Evaluation of osteogenic ability in vivo

At 5 and 9 weeks postoperative, the bone was extracted and scanned with a micro-CT $25\,\mu m$ scanner to observe the erosion of the skull surface. ImageJ was used to calculate the bone defect area of the micro-CT scanning image to judge the erosion of the skull by bacteria and the formation of new bone. Bone infection was assessed using H&E and Giemsa staining, and bone fiber regeneration was assessed using Masson staining.

3 Results and discussion

3.1 Preparation and characterization of the vancomycin-embedded acellular periosteum Van-PEM hydrogel

A hydrogel derived from a decellularized periosteum matrix was prepared, and its microstructure and composition were

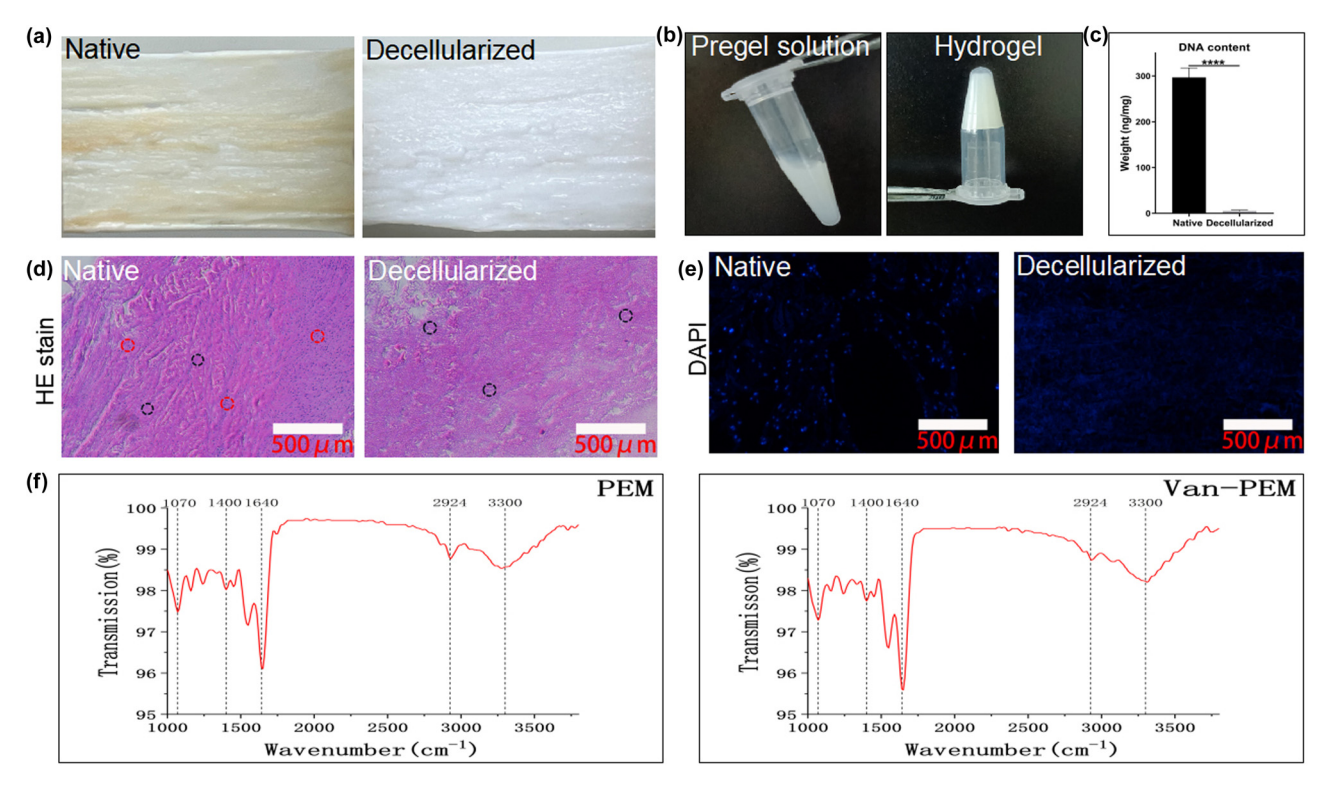


Figure 1: (a) Primary and post-acellular periosteum. (b) Pregel solution under acidic conditions and solid gel under neutral conditions. (c) Changes in the DNA content before and after the acellular process. DNA tests confirmed the removal of the nucleus. (d) H&E staining before and after periosteum decellularization confirms the complete removal of cells (red dashed circles) and the preservation of collagen fibers (black dashed circles). (e) DAPI staining before and after the acellular process. DAPI staining demonstrated that the periosteum was completely removed after acellular treatment. (f) FTIR spectra of the PEM and Van-PEM hydrogels, and it was confirmed that the addition of vancomycin did not react with PEM hydrogel to generate new chemical bonds.

characterized. In addition, bond formation between vancomycin and the hydrogel was assayed. After decellularization, no marked changes in the periosteal tension were observed (Figure 1a). At the same time, it was observed that the vancomycin-loaded hydrogels exhibited flow dynamics under acidic conditions during the preparation process and could be transformed into uniform gel (solid) state after incubation for 5 min at neutral temperature and 37°C (Figure 1b). The DNA content within the periosteum was almost undetectable (native groups vs decellularized groups: $296.7 \pm 20.82 \,\text{ng/mg}$ wet weight vs 5.00 ± 2.00 , p < 0.05, Figure 1c). H&E staining results indicated that the periosteum still possessed a well-organized cambium and fibrous layer structure after cell removal (Figure 1d), which was also confirmed by 4',6-diamino-2-phenylindole staining (DAPI) staining (Figure 1e). These results demonstrate that the structure of the extracellular matrix of the periosteum was preserved after decellularization, which may benefit the preservation of function [30]. The Fourier transform infrared spectra (FTIR) spectra of the PEM and Van-PEM hydrogels showed that the functional groups mainly included OH/NH stretching at 3,300 cm⁻¹, C=N stretching at 1,550 cm⁻¹, C=C stretching at 1,640 cm⁻¹, and C-H stretching at 2,924 cm⁻¹, while the peaks at 1,400 and 1,450 cm⁻¹ corresponded to C-H bending, and the peak at 1,070 cm⁻¹ was attributed to C-O stretching [33]. The addition of vancomycin did not alter the absorption peak of the PEM hydrogel (Figure 1f). This indicated that vancomycin was simply embedded in the hydrogel without any reaction between it and the hydrogel to generate new chemical bonds.

Representative microstructures of the PEM and Van-PEM hydrogels were observed using SEM. The results show that the microstructures of the PEM and Van-PEM hydrogels were three-dimensional nanofiber network (Figure 2a and b). The porosity was calculated using ImageJ software

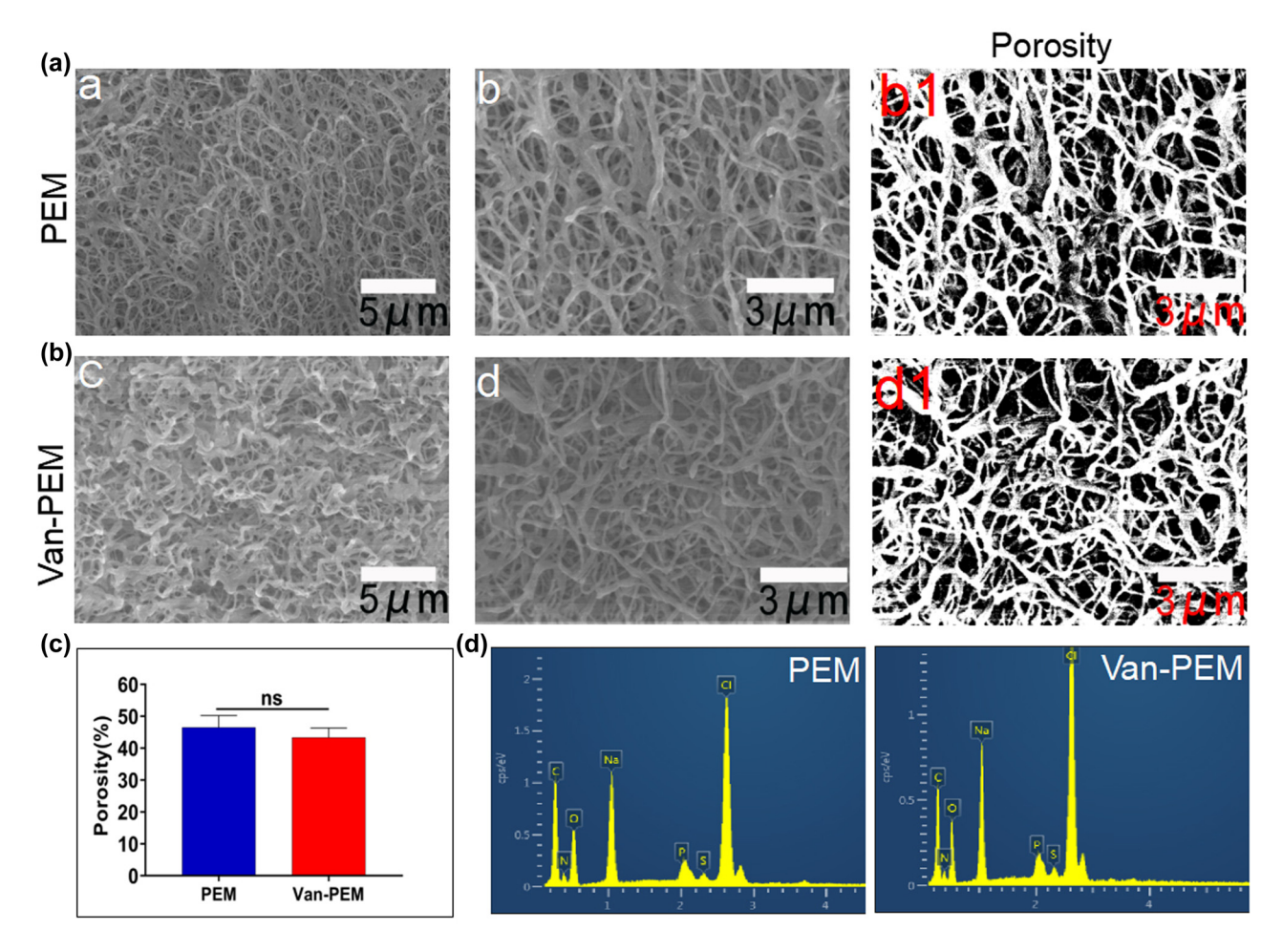


Figure 2: $[(a) \text{ Microstructure of the PEM hydrogel at } 5,000 \times (a) \text{ and } 10,000 \times (b); (b1) \text{ is the condition of } (b) \text{ after ImageJ software processing]}.$ $[(b) \text{ Microstructure of the Van-PEM hydrogel at } 5,000 \times (c) \text{ and } 10,000 \times (d); (d1) \text{ is the condition of } (d) \text{ after ImageJ software processing]}.$ $(c) \text{ Porosities of the PEM and Van-PEM hydrogels calculated by statistical treatment. Meanwhile, the porosities of the PEM and Van-PEM hydrogels exhibited that vancomycin did not significantly change the porosity of PEM hydrogels. <math>(d) \text{ EDS analysis of the PEM and Van-PEM hydrogels}.$

(Figure 2ab1 and bd1), and the PEM hydrogel and Van-PEM hydrogels possessed similar porosities (PEM hydrogel groups vs Van-PEM hydrogel groups: $46.52 \pm 3.715\%$ vs $43.38 \pm 2.957\%$, p > 0.05, Figure 2c), indicating that the addition of vancomycin did not significantly change the porosity of PEM hydrogel. Thus, vancomycin may be embedded in the fiber structure instead of the fiber interstitium. The energy-dispersive X-ray spectroscopy (EDS) results showed that the PEM and Van-PEM hydrogels were mainly composed of C, N, O, Na, P, S, and Cl, in which P is a necessary element for the formation of hydroxyapatite crystals. It can be deposited in the collagen fibers and the nano-interstices between collagen fibers, thus promoting osteoid mineralization into new bone [34] (Figure 2d).

The high porosity of the hydrogels can provide sufficient space for the growth of bone progenitor cells and vascular cells and the storage of vancomycin, all of which greatly contribute to bone reconstruction. An image of the PEM hydrogel after freeze–drying is shown in Figure 3a, demonstrating that the periosteum powder formed a scaffold structure through collagen remodeling. The media immersion results showed no significant difference in porosity between the PEM and Van-PEM hydrogel groups (PEM hydrogel groups vs Van-PEM hydrogel groups: 50.96 \pm 4.824% vs 53.74 \pm 4.048%, p > 0.05, Figure 3b). The porous structure of protein-derived hydrogels is related

to the number of viable cells in the hydrogels, and the larger the voids in the hydrogels, the more the cells in the hydrogel can grow [35]. This may be because appropriate porosity allows nutrient exchange between osteoblasts and hosts [36]. The prepared periosteum hydrogel scaffold presented a 3D network structure with appropriate porosity, which provided sufficient space and nutrition for osteoblasts to survive in the scaffold. The collagen fiber structure provides a carrier for hydroxyapatite crystal deposition, thus accelerating bone reconstruction [37].

In the PBS solution, the degradation behaviors of the PEM and Van-PEM hydrogels were similar and slow. and the percentages of residual mass after 21 days were 59.25 ± 1.659 and $64.09 \pm 1.899\%$, respectively (p > 0.05, Figure 3c). It was also observed that the addition of collagen protease accelerated the degradation rate of the PEM and Van-PEM hydrogels, and the PEM and Van-PEM hydrogels were completely degraded after 5 days (Figure 3d). The PEM or Van-PEM scaffolds are clearly fast-degrading scaffolds, especially in the presence of collagenase (5 days). However, despite the degradation of these scaffolds (dECM, fibrin, and collagen), they are playing a crucial role in bone remodeling. In analogy to the bone remodeling after the fracture, such scaffolds are playing an important role in cell attachment and cell migration [38]. In addition, we found that vancomycin was released slowly

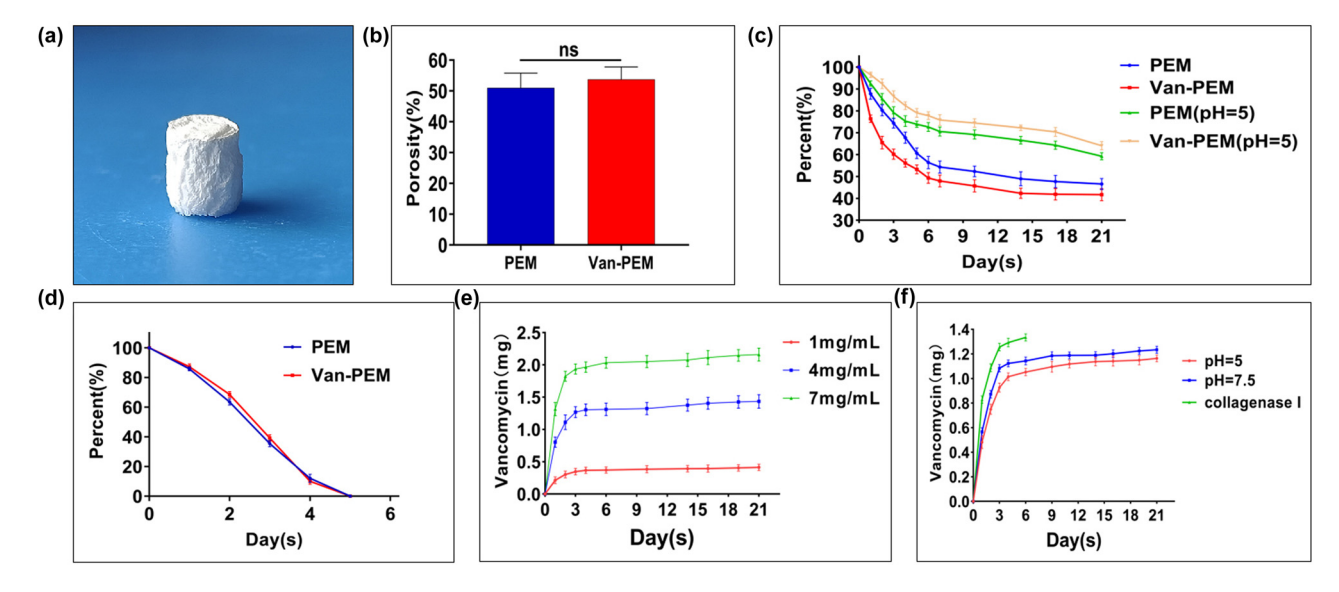


Figure 3: (a) Morphology of the Van-PEM hydrogel after lyophilization. (b) Porosities of the PEM and Van-PEM hydrogels calculated using the immersion method, proving that the addition of vancomycin did not change the porosity of PEM hydrogel. (c) Degradation of the PEM and Van-PEM hydrogels under neutral and acidic conditions exhibited that PEM and Van-PEM hydrogels under neutral and acidic conditions were slowly degraded, and the acidic conditions would not significantly accelerate the degradation of the hydrogel. (d) Degradation of the PEM and Van-PEM hydrogels in the presence of type I collagen protease. (e) Vancomycin release from the Van-PEM hydrogel loaded with vancomycin at different concentrations. (f) Release of vancomycin from the Van-PEM hydrogel loaded with 2 mg/mL vancomycin demonstrated sustained release behavior under acidic or neutral conditions. The type I collagen protease can accelerate the release of vancomycin in Van-PEM hydrogel.

for at least 21 days. The release behavior was similar; the release rate was fastest within the first 3 days, after which it continued more slowly. After 21 days, the percentages of accumulated released vancomycin were 41.4 ± 4.825% (1 mg/mL), $35.86 \pm 2.631\%$ (4 mg/mL), and $30.84 \pm 1.429\%$ (7 mg/mL) (Figure 3e). The vancomycin release behavior of the Van-PEM hydrogel in PBS solution at pH 7.5, PBS solution at pH 5, and type I collagenase solution is presented in Figure 3f. The results showed that the release rate of vancomycin was fastest in the type I collagen solution, and the release rate was slow in PBS solutions with pH of 7.5 and 5. This effectively prevents the rapid release of vancomycin. causing the implant to lose its antibacterial effect and become a carrier for bacterial adhesion [39]. Interestingly, when the Van-PEM hydrogel was completely degraded in type I collagenase, the amount of released vancomycin in the solution was $55.07 \pm 1.47\%$, indicating that when the Van-PEM hydrogel was fully degraded, a large portion of vancomycin remained unreleased. This portion of vancomycin may be physically or electrostatically adsorbed onto the surface by hydrogel fragments [7]. As a result, it will not be released into the solution for metabolism, which is conducive to maintaining continuous sterilization and contact sterilization of the hydrogel. This can maintain the sterile state of the hydrogel scaffold and avoid possible side effects caused by high vancomycin concentrations at the same dose [30]. In addition, the infection can lead to a localized acidic environment, which may accelerate implant degradation, increase osteoclast activity, and decrease osteoblast activity, thereby impeding the repair of bone defects [7,40]. Our study confirmed that acidic conditions do not affect the degradation rate of the Van-PEM hydrogel, which can provide long-term bactericidal action; therefore, it can prevent or improve the local acidic environment and accelerating osteoblast proliferation caused by bacterial infection.

Different concentrations were often used to test the inhibitory effect of the hydrogel on bacteria growth. In this experiment, we selected Van-PEM hydrogel with 2 mg vancomycin in 1 mL PEM hydrogel as the experimental sample. We found that vancomycin in Van-PEM hydrogel exhibited a similar release curve, with a larger proportion released at low concentrations (Figure 3e). Since a high concentration (>3 mg/mL) of vancomycin can inhibit cell growth [7], we believe that 2 mg/mL Van-PEM hydrogel possesses a good drug release effect, which can inhibit the growth of surrounding bacteria and can avoid the side effects caused by a high concentration of vancomycin. Of course, in practical application, we can select different concentrations of vancomycin according to the situation of bone and soft tissue and select sensitive antibiotic according to bacterial culture.

3.2 Antibiotic-loaded PEM hydrogel for the long-term bactericidal effect

The antibacterial activities of the PEM and Van-PEM hydrogels were measured using improved OCM (Figure 4). The results showed that compared with PEM hydrogel, the Van-PEM hydrogel demonstrated a clear antibacterial effect on MRSA (0.16 \pm 0.058 mm vs 15.06 \pm 1.505 mm, p < 0.05, Figure 4a1) and E. faecalis (0.16 \pm $0.066 \text{ mm } vs 18.62 \pm 0.589 \text{ mm}, p < 0.05, \text{ Figure 4b1}) \text{ on}$ the first day. However, as shown in Figure 4c1, when loaded with vancomycin, the bactericidal effect on E. coli was markedly weakened. Therefore, we replaced the vancomycin with amikacin and found that the resulting PEM hydrogel was much more effective against E. coli (0.10 ± $0.01 \,\mathrm{mm} \, vs \, 15.36 \pm 1.001 \,\mathrm{mm}, \, p < 0.05).$

In addition, the Van-PEM hydrogel was immersed in PBS solution that was changed daily. The Van-PEM hydrogel was removed on days 8, 15, and 22 for bacteriostatic zone experiments. The results indicate that the Van-PEM hydrogel exhibited bacteriostatic effects on S. aureus and E. faecalis on days 8, 15, and 22. However, with an increase in time, the antibacterial effect of the Van-PEM hydrogel gradually decreased, and the antibacterial effect on day 22 was significantly weaker than that on the first day (*S. aureus*: $2.35 \pm 0.26 \text{ mm } vs 15.06 \pm 1.505 \text{ mm}$ and *E. faecalis*: 6.12 ± 1.39 mm vs 18.62 ± 0.589 mm, p < 0.05; Figure 4a and b). The PEM hydrogel loaded with amikacin had a similar antibacterial effect on E. coli (Figure 4c), indicating that the PEM hydrogel can provide long-term sustained release of multiple antibiotics, corresponding to the long-term release of vancomycin (Figure 3c and e), and has the potential to carry multiple antibiotics to compensate for the insufficient antibacterial spectrum of a single antibiotic. For example, bone infections caused by open trauma and diabetes often contain gram-positive and gram-negative bacteria [32]. However, PEM hydrogels can only release both drugs simultaneously, and the conditions for the sequential release of controlled-release drugs need to be further explored.

Subsequently, we tested the bacterioplankton-killing performance of PEM and Van-PEM hydrogels using CCM (Figure 4d). The results showed that the number of bacterial colonies on the culture medium of the Van-PEM hydrogel group was significantly lower than that of the PEM hydrogel group. The number of bacterial colonies on the culture medium of the Van-PEM hydrogel group and PEM hydrogel group at 12 h was 1,800 \pm 200 and 6.667 \pm 3.055, respectively. These results further confirm the antibacterial effect of the Van-PEM hydrogel.

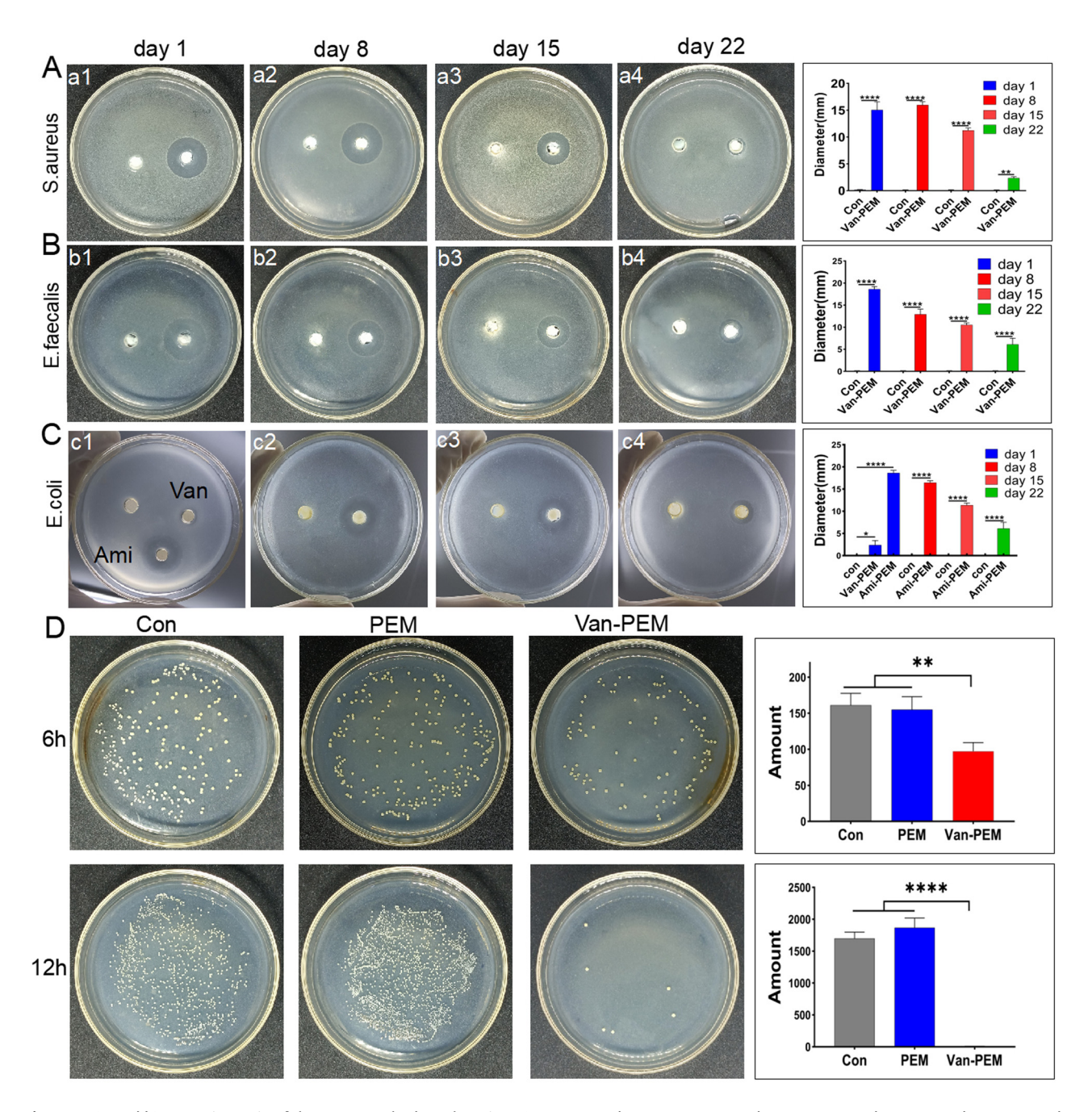


Figure 4: (a and b) Bacteriostasis of the Van-PEM hydrogel against *S. aureus* and Enterococcus on days 1, 8, 15, and 22. It was demonstrated that Van-PEM hydrogel was still able to kill gram-positive bacteria on day 22. (c) Bacteriostasis of the Ami-PEM hydrogel against *E. coli* on days 1, 8, 15, and 22. (d) Bacterioplankton killing abilities of the PEM and Van-PEM hydrogels.

3.3 Biocompatibility of PEM and Van-PEM hydrogels

The cytotoxicity of bone marrow MSCs cultured with PEM and Van-PEM hydrogels was investigated. After 48 h of co-culture, calcein staining showed no significant difference in the number of living cells among the blank, PEM, and Van-PEM hydrogel groups (Figure 5a). ImageJ software

was used to evaluate the area of green fluorescence representing living cells in Figure 5a. The results showed that the fluorescence areas in the control, PEM, and Van-PEM hydrogel groups were similar (Figure 5b), confirming that the PEM and Van-PEM hydrogels were not significantly cytotoxic to MSCs.

Additionally, the cellular metabolic activity was determined using the CCK-8 assay to analyze the cytotoxicity of

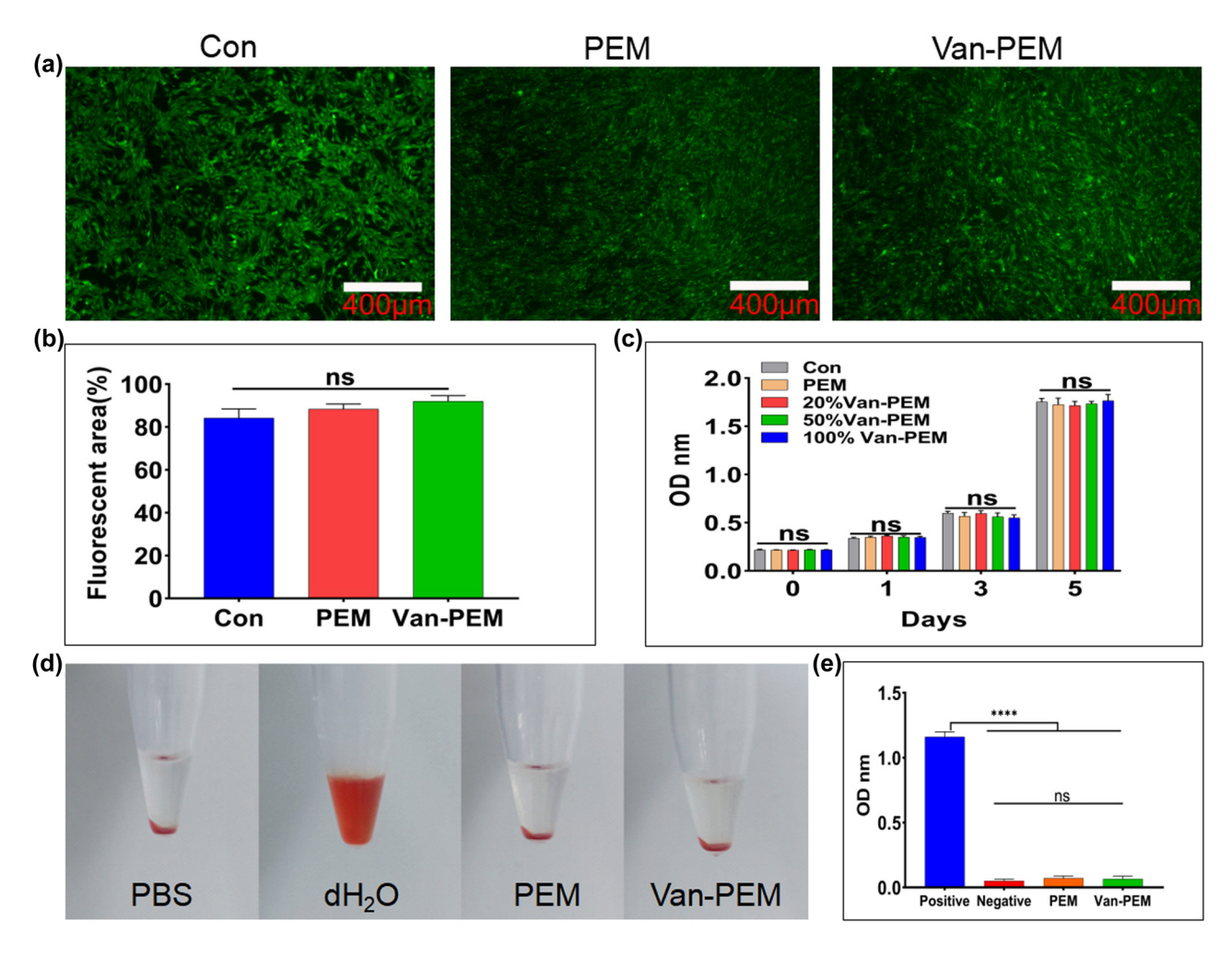


Figure 5: (a) Calcein staining after co-culture of the PEM and Van-PEM hydrogels with BMSCs. (b) Fluorescence staining areas in (a) calculated using ImageJ software. (c) BMSCs cultured with PEM hydrogel and Van-PEM hydrogel extracts of different concentrations. (d) Hemolysis reactions of PEM and Van-PEM hydrogels. PEM and Van-PEM hydrogels do not cause hemolysis. (e) Absorbance of hemoglobin in the supernatant of (d).

the PEM hydrogel and Van-PEM hydrogel immersion solutions. As shown in Figure 5c, the reproduction of cells in the blank group, PEM group, and 25, 50, and 100% Van-PEM hydrogel immersion groups displayed no significant differences on days 1, 3, and 5 (p > 0.05), and the number of cells on day 5 was significantly increased in all groups. Thus, the PEM and Van-PEM hydrogels did not induce significant toxicity in the MSCs. Previous studies have demonstrated that high concentrations of vancomycin have toxic effects on cells [30]. Our results suggest that Van-PEM hydrogel is beneficial for reducing the cytotoxicity of vancomycin.

During the preparation of PEM and Van-PEM hydrogels, Triton X-100, which causes a hemolytic reaction [41], is needed. Therefore, it is necessary to conduct blood compatibility testing on PEM and Van-PEM hydrogels. Suspended human red blood cells were used to detect hemolysis reactions in the PEM and Van-PEM hydrogels. As shown in Figure 5d,

dH₂O dissolved almost all the red blood cells, producing a red supernatant, whereas there was no detectable red color in the supernatant of the PBS, PEM, and Van-PEM hydrogel groups. The hemolytic activity was further quantified using a UV spectrophotometer (Figure 5e). These results showed that there was almost no hemoglobin in the supernatant of the PEM hydrogel and Van-PEM hydrogel groups, indicating almost no residual chemical reagents in the PEM and Van-PEM hydrogels, which had good blood compatibility.

3.4 Osteogenesis induced by PEM and Van-**PEM hydrogels**

Osteoblasts can promote bone formation through bone matrix deposition, and ALP can be used as a marker for early mineralization [42]. The osteogenic differentiation

Qi Dong et al.

of MC3T3-E1 cells on the PEM and Van-PEM hydrogels was evaluated by measuring the ALP activity (Figure 6a). On the day 3, there was no significant difference in ALP activity among the control, PEM, and Van-PEM hydrogel groups. On day 7, compared with the control group, the ALP activity of the PEM hydrogel and Van-PEM hydrogel groups increased significantly. In addition, ALP staining on day 7 showed that the staining depth of the PEM and Van-PEM hydrogel groups was greater than that of the control group (Figure 6b and Figure S1). ALP results confirmed the ability of the Van-PEM hydrogel to promote bone formation.

Additionally, the expression of osteogenic genes, such as Runx2, OSX, and OCN, in MC3T3-E1 cells was determined by RT-PCR after 14 days of co-culture with PEM and Van-PEM hydrogels (Figure 6c-e). The results showed that the PEM and Van-PEM hydrogels could significantly promote gene expression in osteoblasts, especially the OSX and OCN genes. These results suggested that the Van-PEM hydrogel with a 3D structure can promote the expression of ALP and osteogenic genes in osteoblasts. Van-PEM hydrogels can increase the degree

of osteogenic differentiation, which is consistent with the finding that fibrin hydrogels can promote osteogenic differentiation of bone marrow MSCs [43]. A possible reason may be that some cytokines (such as osteoprotegerin) in hydrogels derived from the periosteum extracellular matrix inhibit osteoclast activity [44]. Moreover, collagen promotes osteoblast activity [45]. The Van-PEM hydrogel can also promote the expression of osteogenic genes in osteoblasts compared to the PEM hydrogel, suggesting that vancomycin does not influence the osteogenic effect of the PEM hydrogel.

3.5 Antibacterial and osteogenic functions of the Van-PEM hydrogel *in vivo*

The model preparation for infectious bone defects in rats is shown in Figure 7a. Micro-CT at 1 week postoperatively showed serious irregular bone erosion areas at the edge of the infectious bone defects, indicating that the infectious bone defect model was successfully prepared (Figure 7b). Micro-CT at 5 weeks postoperatively showed

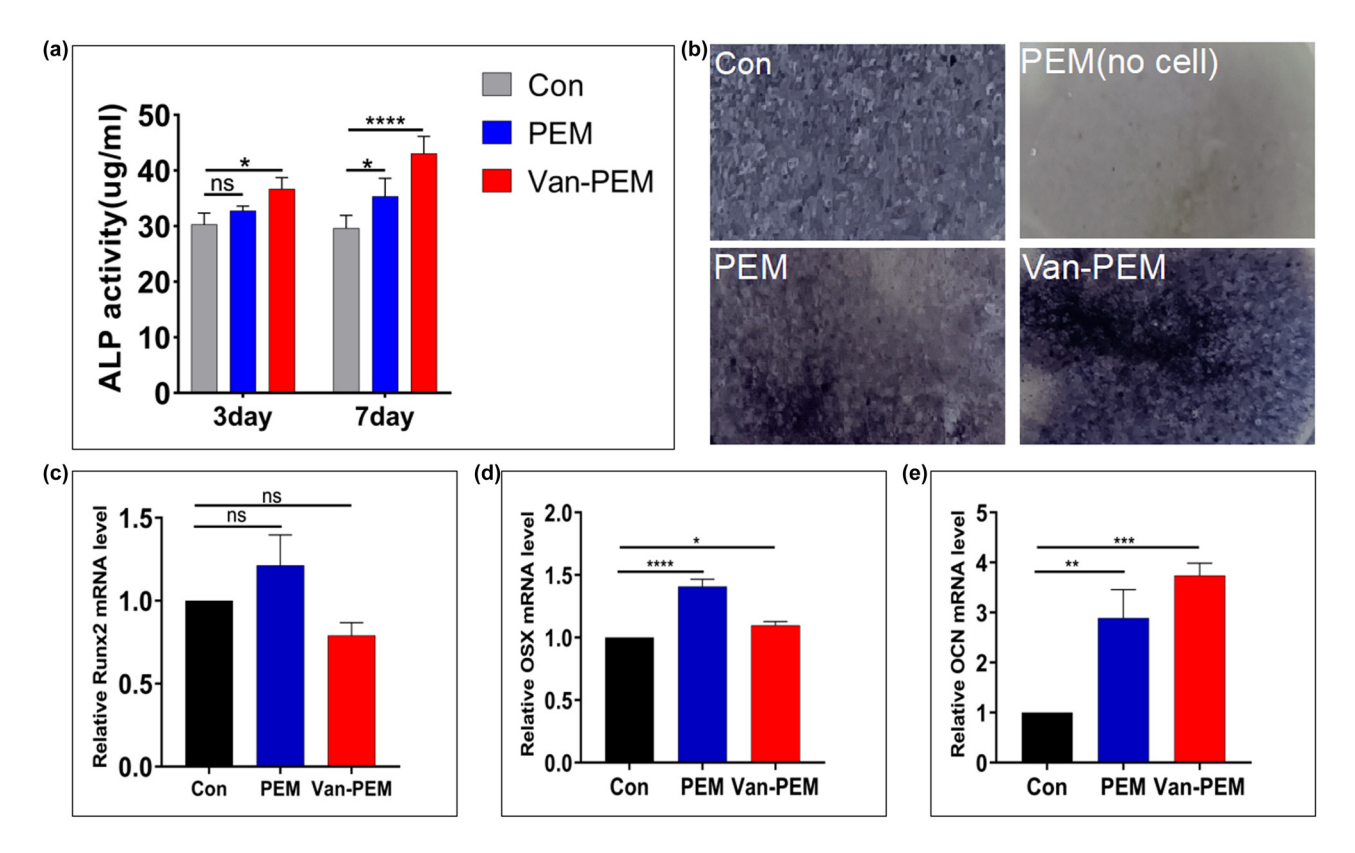


Figure 6: (a) Secretion of ALP by osteoblasts in the PEM and Van-PEM hydrogels. PEM and Van-PEM hydrogels can promote the secretion of ALP from osteoblasts. (b) ALP staining of osteoblasts cultured in the PEM and Van-PEM hydrogels for 7 days. (c-e) Expression of osteogenic genes Runx2, OSX, and OCN detected by RT-PCR in osteoblasts cultured in PEM and Van-PEM hydrogels for 14 days. Van-PEM hydrogels can significantly promote the expression of OCN.

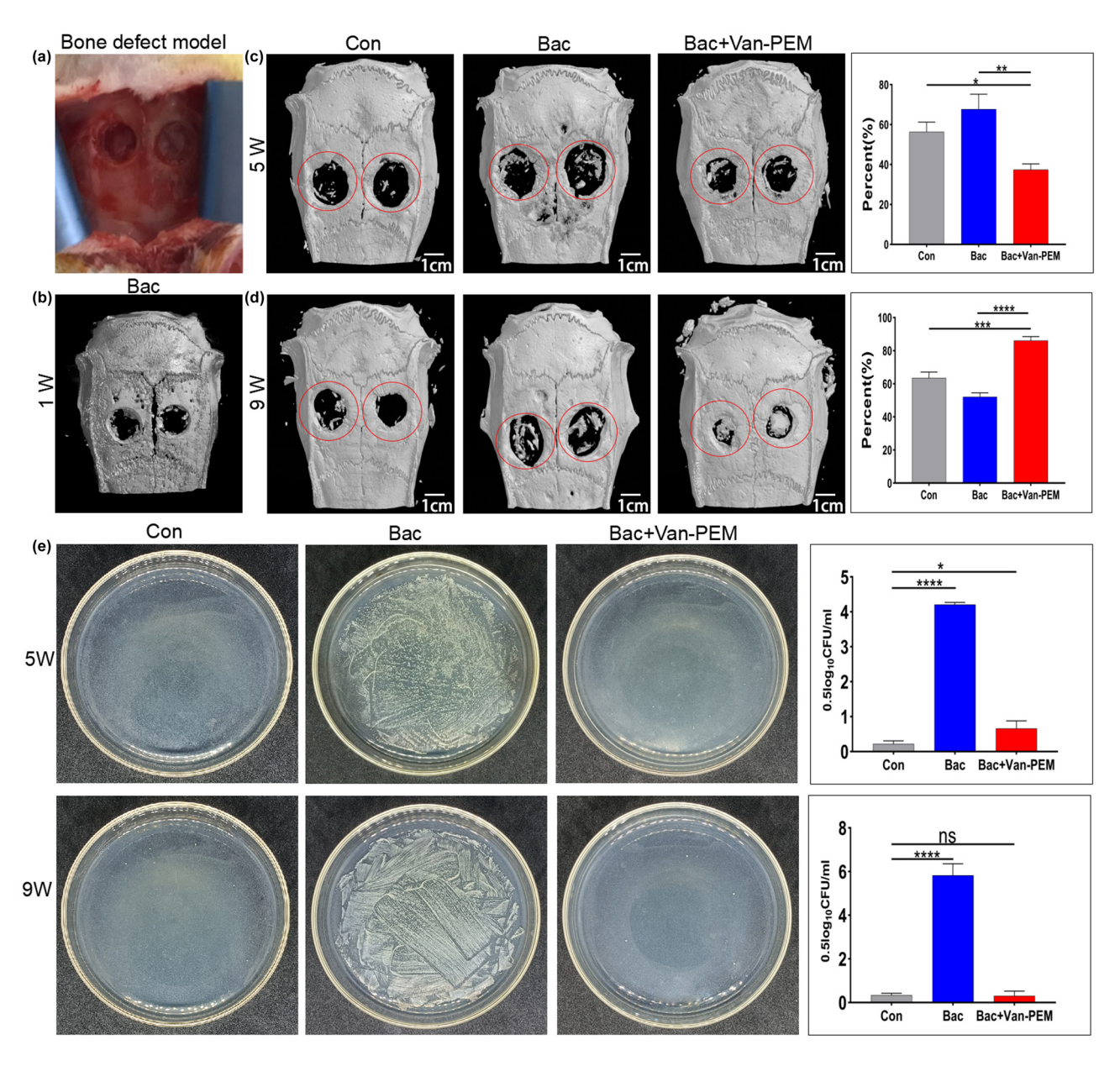


Figure 7: (a) Gross picture of the infectious skull defect model. (b) Micro-CT image of infection defect model 1 week after surgery. (c) Degree of skull erosion detected by micro-CT at 5 weeks after surgery. (d) Bone regeneration in the skull defect detected by micro-CT at 9 weeks after surgery. (e) Bacterial growth in the skull wounds of the control, bacteria-treated, and Van-PEM groups at 5 and 9 weeks after surgery.

that the erosion area of the skull defect edge in the Van-PEM hydrogel-treated group was significantly smaller than that in the control and bacteria-treated groups. The quantitative results demonstrated that the erosion areas of skull defects in the Van-PEM, control, and bacteria-treated groups were 37.42 ± 2.89 , 56.36 ± 4.87 , and $67.71 \pm 7.54\%$, respectively (Figure 7c). At 9 weeks postoperatively, micro-CT indicated that the Van-PEM hydrogel-treated group possessed significantly more new bone formation than the control or bacteria-treated groups, and the bone regeneration rate (bone mass/total volume in the red circle, BV/TV) was

more than 70%. The osteogenic capacity of the bacteria-treated group was slightly lower than that of the control group. Bone regeneration ratios were 52.11 \pm 2.41 and 63.51 \pm 3.58%, respectively (Figure 7d). The aforementioned results suggest that infection reduces bone-forming ability and that the Van-PEM hydrogel can improve bone-forming ability. The number of bacteria at the infected sites in the blank, bacteria-treated, and Van-PEM hydrogel groups was measured using the diffusion plate method at 5 and 9 weeks after surgery (Figure 7e). The results showed that the number of bacterial colonies in the culture dish of

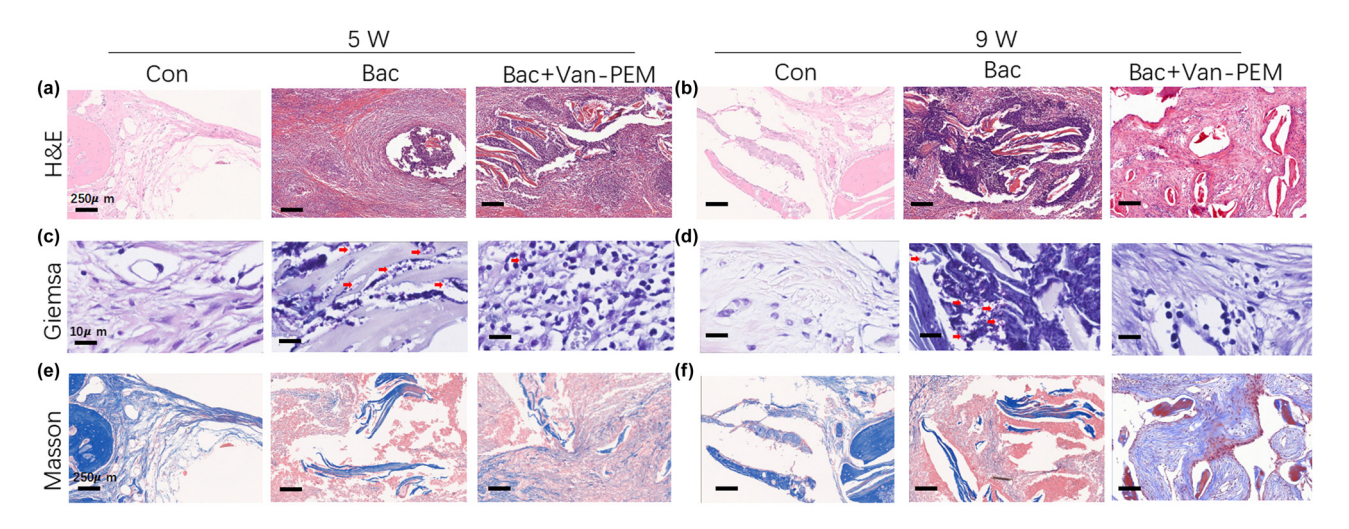


Figure 8: (a and b) H&E staining of the skull wounds in the control, bacteria-treated, and Van-PEM groups at weeks 5 and 9. Van-PEM hydrogel treatment can significantly reduce the inflammatory response. (c and d) Giemsa staining of each group at the same time points. Van-PEM hydrogel can reduce the number of bacteria in the bone defect site. Red arrows indicate bacteria hidden in tissue. (e and f) Masson staining of each group at the same time points. Van-PEM hydrogel treatment promotes collagen formation.

the bacteria-treated group was much higher than that of the control and Van-PEM hydrogel groups.

H&E, Giemsa, and Masson's trichrome staining schemes were used to determine the anti-infection and osteogenic effects of the hydrogels. At week 5, the number of neutrophils in bone tissue in the bacteria-treated and Van-PEM hydrogel-treated groups was greater than that in the control group (Figure 8a), while the number in the Van-PEM hydrogeltreated group decreased significantly at week 9. An increasing trend was observed in the bacteria-treated group (Figure 8b). Giemsa staining was performed to observe bacteria present in the bone tissue. At Week 5, many bacteria were observed in the bacteria-treated group, whereas the number of bacteria in the control and Van-PEM-treated groups was relatively small (red arrow, Figure 8c). At week 9, many bacteria were still found in the bacteria-treated group, whereas the number of bacteria in the Van-PEM-treated group was significantly reduced (red arrow, Figure 8d). Masson's trichrome staining showed that a large number of new bones were formed in the Van-PEM hydrogel group, most of which were cancellous bones with complete mineralization of collagen (dyed blue), whereas in the blank and bacteria-treated groups, it was mostly unmineralized collagen (Figure 8e and f).

4 Conclusions

We prepared a novel biomaterial with antibacterial and osteogenic properties by physically embedding vancomycin into an acellular perichondrium hydrogel. The Van-PEM hydrogel possesses a three-dimensional structure with high porosity. For *in vitro* experiments, the sustained release of a variety of antibiotics, long-term bactericidal properties, bone induction, and osteogenesis ability, and good biocompatibility were demonstrated. Finally, it was confirmed that the Van-PEM hydrogel could kill bacteria for a long period and promote the regeneration of bone tissue in infectious skull defects in a rat model. Therefore, Van-PEM hydrogels have broad prospects for the treatment of infectious bone defects.

Funding information: This work was supported by the Natural Science Foundation of Zhejiang Province (grants LBY22H180007 and LBY22H270004) and the Medical and Health Science and Technology Plan Project of Zhejiang Province (grants 2020KY990 and 2022KY416).

Author contributions: Qi Dong is responsible for the preparation of antibacterial gel and the writing of articles; Sunfang Chen is responsible for the physical characterization of the gel; Jiuqin Zhou is responsible for histological detection; Jingcheng Liu and Yubin Zou are responsible for animal experiments; Jiawei Lin and Jun Yao are responsible for the osteogenic performance experiment of antibacterial gel; Dan Cai is responsible for bacterial experiments; Danhua Tao and Bing Wu are responsible for processing experimental data and assisting in the writing of articles; and Bin Fang is responsible for the design and management of the whole experiment. All authors have accepted responsibility for the entire content of this manuscript and approved its submission.

Conflict of interest: The authors state no conflict of interest.

Ethical approval: The research related to animals' use has been complied with all the relevant national regulations and institutional policies for the care and use of animals.

Data availability statement: The datasets generated during and/or analyzed during the current study are available from the corresponding author on reasonable request.

References

- Wang Y, Jiang H, Deng Z, Jin J, Meng J, Wang J, et al. Comparison of monolateral external fixation and internal fixation for skeletal stabilisation in the management of small tibial bone defects following successful treatment of chronic osteomyelitis. Biomed Res Int. 2017;2017:6250635.
- Sun A, Lin X, Xue Z, Huang J, Bai X, Huang L, et al. Facile surface functional polyetheretherketone with antibacterial and immunoregulatory activities for enhanced regeneration toward bacterium-infected bone destruction. Drug Deliv. 2021;28(1):1649-63.
- Korean Society for Chemotherapy, Korean Society of Infectious Diseases, Korean Orthopaedic Association. Clinical guidelines for the antimicrobial treatment of bone and joint infections in Korea. Infect Chemother. 2014;46(2):125-38.
- Zwingenberger S, Nich C, Valladares RD, Yao Z, Stiehler M, Goodman SB. Recommendations and considerations for the use of biologics in orthopedic surgery. BioDrugs. 2012;26(4):245-56.
- Freischmidt H, Armbruster J, Rothhaas C, Titze N, Guehring T, Nurjadi D, et al. Treatment of infection-related non-unions with bioactive glass-a promising approach or just another method of dead space management? Mater (Basel). 2022;15(5):1697.
- Goldberg VM, Akhavan S. Biology of bone grafts, in bone regeneration and repair: Biology and clinical applications. In Lieberman JR, Friedlaender GE, editors. Totowa, NJ: Humana Press; 2005. p. 57-65.
- Fang B, Qiu P, Xia C, Cai D, Zhao C, Chen Y, et al. Extracellular matrix scaffold crosslinked with vancomycin for multifunctional antibacterial bone infection therapy. Biomaterials. 2021;268:120603.
- [8] Budiatin AS, Gani MA, Samirah, Ardianto C, Raharjanti AM, Septiani I, et al. Bovine hydroxyapatite-based bone scaffold with gentamicin accelerates vascularization and remodeling of bone defect. Int J Biomater. 2021;2021:5560891.
- Kojima KE, de Andrade ESFB, Leonhardt MC, de Carvalho VC, de Oliveira PRD, Lima A, et al. Bioactive glass S53P4 to fill-up large cavitary bone defect after acute and chronic osteomyelitis treated with antibiotic-loaded cement beads: A prospective case series with a minimum 2-year follow-up. Injury. 2021;52(Suppl 3):S23-8.
- [10] Qiu G, Huang M, Liu J, Wang P, Schneider A, Ren K, et al. Antibacterial calcium phosphate cement with human

- periodontal ligament stem cell-microbeads to enhance bone regeneration and combat infection. J Tissue Eng Regen Med. 2021;15(3):232-43.
- Yuan J, Wang B, Han C, Huang X, Xiao H, Lu X, et al. Nanosized-Ag-doped porous β -tricalcium phosphate for biological applications. Mater Sci Eng C Mater Biol Appl. 2020;114:111037.
- Qiu X, Li S, Li X, Xiao Y, Li S, Fen Q, et al. Experimental study of β-TCP scaffold loaded with VAN/PLGA microspheres in the treatment of infectious bone defects. Colloids Surf B Biointerfaces. 2022;213:112424.
- [13] Zeng Y, Hoque J, Varghese S. Biomaterial-assisted local and systemic delivery of bioactive agents for bone repair. Acta Biomater, 2019:93:152-68.
- [14] Liu YZ, Li Y, Yu XB, Liu LN, Zhu ZA, Guo YP. Drug delivery property, bactericidal property and cytocompatibility of magnetic mesoporous bioactive glass. Mater Sci Eng C Mater Biol Appl. 2014;41:196-205.
- [15] Kargozar S, Montazerian M, Hamzehlou S, Kim HW, Baino F. Mesoporous bioactive glasses: Promising platforms for antibacterial strategies. Acta Biomater. 2018;81:1-19.
- [16] Schnürer SM, Gopp U, Kühn KD, Breusch SJ. Bone substitutes. Orthopade. 2003;32(1):2-10.
- Dos Santos DA, de Guzzi Plepis AM, da Conceição Amaro Martins V, Cardoso GBC, Santos AR Jr., Iatecola A, et al. Effects of the combination of low-level laser therapy and anionic polymer membranes on bone repair. Lasers Med Sci. 2020;35(4):813-21.
- Wolf MT, Daly KA, Brennan-Pierce EP, Johnson SA, Carruthers CA, D'Amore A, et al. A hydrogel derived from decellularized dermal extracellular matrix. Biomaterials. 2012;33(29):7028-38.
- [19] DeQuach JA, Yuan SH, Goldstein LS, Christman KL. Decellularized porcine brain matrix for cell culture and tissue engineering scaffolds. Tissue Eng Part A. 2011;17(21-22):2583-92.
- [20] Singelyn JM, DeQuach JA, Seif-Naraghi SB, Littlefield RB, Schup-Magoffin PJ, Christman KL. Naturally derived myocardial matrix as an injectable scaffold for cardiac tissue engineering. Biomaterials. 2009;30(29):5409-16.
- [21] Farnebo S, Woon CY, Schmitt T, Joubert LM, Kim M, Pham H, et al. Design and characterization of an injectable tendon hydrogel: A novel scaffold for guided tissue regeneration in the musculoskeletal system. Tissue Eng Part A. 2014;20(9-10):1550-61.
- [22] Zhang W, Wang N, Yang M, Sun T, Zhang J, Zhao Y, et al. Periosteum and development of the tissue-engineered periosteum for guided bone regeneration. J Orthop Transl. 2022;33:41-54.
- da Luz Moreira P, Genari SC, Goissis G, Galembeck F, An YH, Santos AR, Jr. Bovine osteoblasts cultured on polyanionic collagen scaffolds: an ultrastructural and immunocytochemical study. J Biomed Mater Res B Appl Biomater. 2013;101(1):18-27.
- [24] Ren H, Lian X, Niu B, Zhao L, Zhang Q, Huang D, et al. The study of mechanical and drug release properties of the mineralized collagen/polylactic acid scaffold by tuning the crystalline structure of polylactic acid. J Biomater Sci Polym Ed. 2021;32(6):749-62.

- [25] Lin X, Zhao C, Zhu P, Chen J, Yu H, Cai Y, et al. Periosteum extracellular-matrix-mediated acellular mineralization during bone formation. Adv Healthc Mater. 2018;7(4):1700660.
- [26] Chen K, Lin X, Zhang Q, Ni J, Li J, Xiao J, et al. Decellularized periosteum as a potential biologic scaffold for bone tissue engineering. Acta Biomater. 2015;19:46–55.
- [27] Zhao L, Zhao J, Tuo Z, Ren G. Repair of long bone defects of large size using a tissue-engineered periosteum in a rabbit model. J Mater Sci Mater Med. 2021;32(9):105.
- [28] Qiu P, Li M, Chen K, Fang B, Chen P, Tang Z, et al. Periosteal matrix-derived hydrogel promotes bone repair through an early immune regulation coupled with enhanced angio- and osteogenesis. Biomaterials. 2020;227:119552.
- [29] Inzana JA, Schwarz EM, Kates SL, Awad HA. Biomaterials approaches to treating implant-associated osteomyelitis. Biomaterials. 2016;81:58-71.
- [30] Cai D, Chen S, Wu B, Chen J, Tao D, Li Z, et al. Construction of multifunctional porcine acellular dermal matrix hydrogel blended with vancomycin for hemorrhage control, antibacterial action, and tissue repair in infected trauma wounds. Mater Today Bio. 2021;12:100127.
- [31] Tabassum S, Ahmad S, Rehman Khan KU, Tabassum F, Khursheed A, Zaman QU, et al. Phytochemical profiling, antioxidant, anti-inflammatory, thrombolytic, hemolytic activity in vitro and in silico potential of Portulacaria afra. Molecules. 2022;27(8):2377.
- [32] Rupp M, Bärtl S, Lang S, Walter N, Alt V. Fracture-related infections after intramedullary nailing: Diagnostics and treatment. Unfallchirurg. 2022;125(1):50–8.
- [33] Masood N, Ahmed R, Tariq M, Ahmed Z, Masoud MS, Ali I, et al. Silver nanoparticle impregnated chitosan-PEG hydrogel enhances wound healing in diabetes induced rabbits. Int J Pharm. 2019;559:23–36.
- [34] Murshed M. Mechanism of bone mineralization. Cold Spring Harb Perspect Med. 2018;8(12):a031229.
- [35] Catelas I, Sese N, Wu BM, Dunn JC, Helgerson S, Tawil B. Human mesenchymal stem cell proliferation and osteogenic differentiation in fibrin gels in vitro. Tissue Eng. 2006;12(8):2385–96.

- [36] Wang M, Li H, Yang Y, Yuan K, Zhou F, Liu H, et al. A 3D-bioprinted scaffold with doxycycline-controlled BMP2-expressing cells for inducing bone regeneration and inhibiting bacterial infection. Bioact Mater. 2021;6(5):1318–29.
- [37] Wu L, Wang Q, Li Y, Yang M, Dong M, He X, et al. A dopamine acrylamide molecule for promoting collagen biomimetic mineralization and regulating crystal growth direction. ACS Appl Mater Interfaces. 2021;13(33):39142-56.
- [38] Anselme K. Osteoblast adhesion on biomaterials. Biomaterials. 2000;21(7):667-81.
- [39] Arciola CR, Campoccia D, Montanaro L. Implant infections: adhesion, biofilm formation and immune evasion. Nat Rev Microbiol. 2018;16(7):397-409.
- [40] Pearson JJ, Gerken N, Bae C, Lee KB, Satsangi A, McBride S, et al. In vivo hydroxyapatite scaffold performance in infected bone defects. J Biomed Mater Res B Appl Biomater. 2020;108(3):1157–66.
- [41] Momtahan N, Panahi T, Poornejad N, Stewart MG, Vance BR, Struk JA, et al. Using hemolysis as a novel method for assessment of cytotoxicity and blood compatibility of decelularized heart tissues. ASAIO J. 2016;62(3):340-8.
- [42] Oezel L, Büren C, Scholz AO, Windolf J, Windolf CD. Effect of antibiotic infused calcium sulfate/hydroxyapatite (CAS/HA) insets on implant-associated osteitis in a femur fracture model in mice. PLoS One. 2019;14(3):e0213590.
- [43] Hou T, Xu J, Li Q, Feng J, Zen L. In vitro evaluation of a fibrin gel antibiotic delivery system containing mesenchymal stem cells and vancomycin alginate beads for treating bone infections and facilitating bone formation. Tissue Eng Part A. 2008;14(7):1173–82.
- [44] Cao Z, Jiang D, Yan L, Wu J. In vitro and in vivo osteogenic activity of the novel vancomycin-loaded bone-like hydroxyapatite/poly(amino acid) scaffold. J Biomater Appl. 2016;30(10):1566-77.
- [45] Labbaf S, Tsigkou O, Müller KH, Stevens MM, Porter AE, Jones JR. Spherical bioactive glass particles and their interaction with human mesenchymal stem cells in vitro. Biomaterials. 2011;32(4):1010-8.